OL Organic Letters

Flux-Screened Copper/Electric Dual-Catalyzed Chemo- and Enantioselective Ullmann-Type C–C Coupling Reactions

Yun Zou, Jia Xin, Yunhe Jin,* and Shengyang Tao*

Cite This: *Org. Lett.* 2024, 26, 9022–9027 Read Online

ABSTRACT: This study introduces an innovative copper/electric dual-catalyzed approach to Ullmann coupling reactions. Our research delineates a series of chemoselective cross-couplings among various halogenated aromatics and enantioselective couplings involving halogenated aryl aldehydes. We employed a flux screening technique to refine the reaction parameters, which is rarely reported in the field of electrochemical synthesis. This advancement accelerates the determination of optimal reaction conditions and affords some inspiration for developing sustainable and ecofriendly chemical synthesis.

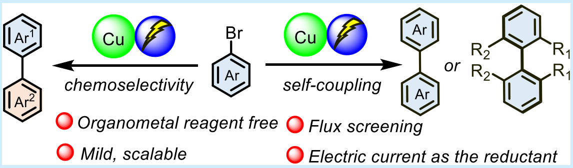

Biaryl compounds are ubiquitous in natural products[1] and serve as pivotal ligands in transition metal catalysis[2] and foundational elements in constructing organic polymer materials.[3] The synthesis of these compounds primarily depends on strategies such as the coupling between organometallic reagents and aryl halides, exemplified by the Suzuki coupling,[4] the direct oxidative coupling of aromatic substrates,[5] and the reductive coupling of aryl halides.[6] Ullmann coupling reaction is a relatively efficient halogenated aromatic reduction coupling reaction discovered earlier (Scheme 1a).[7] However, it is not without its challenges, such as the necessity for high reaction temperatures and the inevitable use of stoichiometric reducing agents. Over the next few decades, chemists catalyzed the reaction by using low-cost metals such as Cu(I) and Ni(0), allowing it to take place at much lower temperatures.[8] In addition, how to realize the cross-coupling of halogenated aromatics is a topic worth studying. Recent studies have incrementally shed light on this domain, as exemplified by the work of Yin et al. in 2021, which demonstrated a nickel-catalyzed chemoselective coupling of halogenated aromatics with equivalent zinc as a reducing agent (Scheme 1b, left).[9] In addition, the use of the Ullmann coupling strategy to achieve the synthesis of chiral biaryl compounds is also worth studying. In 2010, Lin et al. unveiled a strategy for enantioselective homocoupling of halogenated aromatics via nickel catalysis, resulting in a chiral biaryl compound (Scheme 1b, right).[10] In addition to the study of selectivity, avoiding or reducing the use of metal-reducing agents is also very important. Electrocatalysis is clean and environmentally sustainable, thus avoiding the use of equivalent reducing agents, so it has great application potential in this field, especially in cross-electrophile coupling reactions.[11] In recent years, studies on nickel/electric collaborative catalysis have been reported one after another.[12] However, copper, the metal that catalyzed Ullman coupling in the first place, has hardly been combined with electric reduction to achieve such reactions. Yet, the scalability of reactions is curtailed by constraints in reaction apparatus and conditions, pacing the progress in electrochemical synthesis research. In this context, using the flux screening method, we disclose our investigation into the electrocopper synergistic catalysis of the Ullmann coupling reaction. A commercial 24-well electrochemical reaction unit that allows a large number of conditional screenings in a relatively short period of time was employed to determine the optimal reaction conditions for three types of couplings,[13]

Scheme 1. Biaryl Synthesis via Cross-Coupling

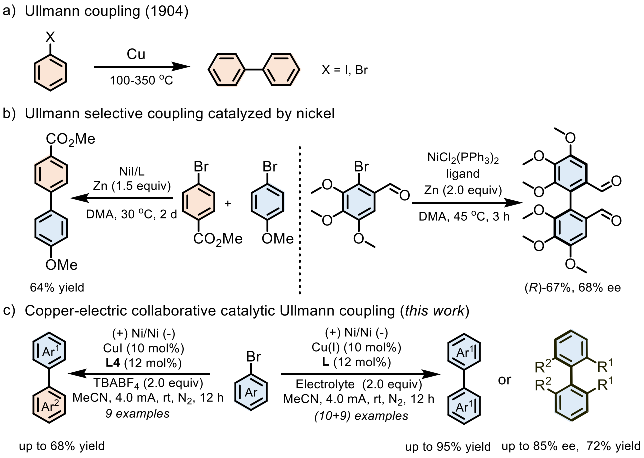

Received: August 28, 2024
Revised: September 19, 2024
Accepted: September 26, 2024
Published: September 30, 2024

https://doi.org/10.1021/acs.orglett.4c03196

including chemically selective cross-coupling of heterologous aryl halides, self-coupling of halogenated aromatics, and enantioselective homocoupling of halogenated aryl aldehydes (Scheme 1c).

In our experiment, we first used CuCl as the catalyst to obtain the self-coupling products of halogenated aromatic hydrocarbogens with a 24-well electrochemical reactor. Some representative results were selected and plotted to display the condition-optimizing procedure (Scheme 2). When the electrode current was screened, the maximum yield of the reaction could reach 60% with a Ni/Ni pair as the anode and cathode of the reaction under a current of 4.0 mA (Scheme 2B). Taking this as the base condition, different catalysts and solvents were then tested, showing the combination of acetonitrile and CuCl to be a good choice. $Cu(MeCN)_4BF_4$ as the catalyst can also give a competitive yield (Scheme 2C). Subsequently, CuCl and $Cu(MeCN)_4BF_4$ were utilized as the catalysts to examine the ligands. It can be determined that the effect of bidentate nitrogen ligands **L4** and **L8** prepared from a bipyridine skeleton is better than that of phosphine ligands and single dentate nitrogen ligands (Scheme 2D). Finally, the above two groups of the ligand and catalyst were combined to explore the added electrolyte. As a result, the best yield of up to 92% was provided with CuCl as the catalyst, **L4** as the ligand, $TBABF_4$ as the electrolyte, acetonitrile as the solvent, and Ni/Ni as the anode and cathode of the reaction under the current of 4.0 mA, room temperature, and nitrogen atmosphere for 12 h.

After the optimal conditions were established, the substrate scope was extended. As shown in Scheme 3, the reaction exhibited good functional group tolerance on a myriad of substitutions including alkyl (**4**, **11**), cyano (**5**, **10**, **12**), trifluoromethyl (**6**), ester (**7**), methoxy (**8**, **9**), and aldehyde (**13**) groups. In the process of scope expansion, different types of functional groups and their positions were found to have a great impact on the reaction; therefore, it is necessary to change the added catalyst to obtain a satisfying yield. With a matching catalyst, the yield of the self-coupling product can reach up to 95% (**11**). The specific matching mechanism was further studied in our lab.

Encouraged by the high efficiency of the electrocatalytic self-coupling reaction, we then turned our focus to the cross-coupling of different halogenated hydrocarbons. To obtain the best selectivity, a niche-targeting optimization was carried out with our flux screening strategy. Some representative results were selected to draw a graph (Scheme 4). According to the optimization results, when the reaction was carried out with CuI as the catalyst, **L4** as the ligand, $TBABF_4$ as the electrolyte, and acetonitrile as solvent at room temperature and a nitrogen atmosphere for 12 h, the maximum yield of the target cross-coupling product could reach 59% with 6.2:1 chemoselectivity.

Subsequently, the substrate scope of this cross-coupling protocol was also investigated (illustrated in Scheme 5). By substitution of electron-withdrawing functional groups, including ester and trifluoromethyl groups, on substrates, a slight increase in the yield of the cross-coupling products (**15** and **16**, up to 68%) was observed, whereas replacing them with methyl groups led to a noticeable decrease in yield (**17**, 33%). When the substituents were all electron-withdrawing, the yield of the products also significantly decreased (**18**). Meanwhile, altering the position of the functional groups was proved to have minimal impact on the reaction outcomes (**20**−**22**). Besides,

Scheme 2. Optimization of Ullmann-Type Self-Coupling[a,b]

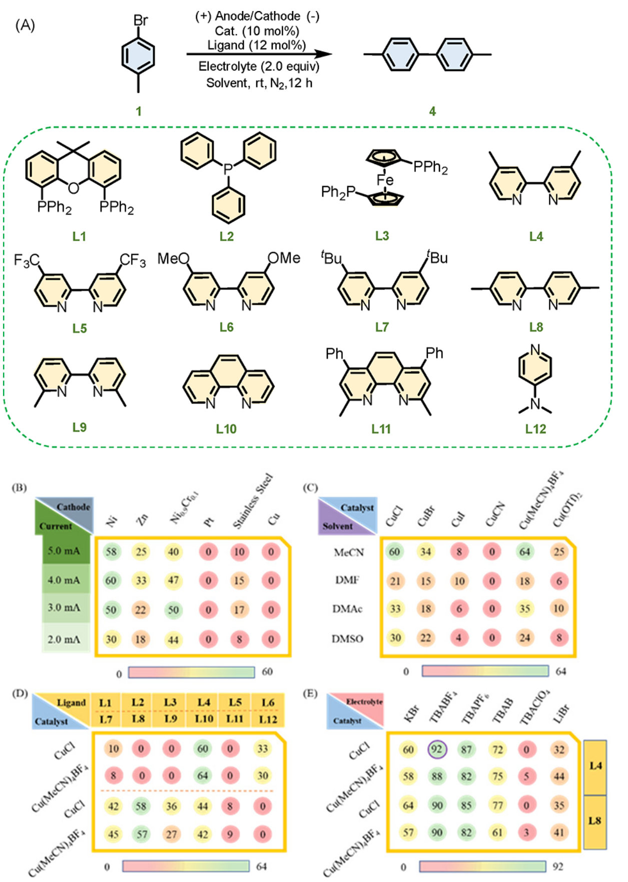

Current \ Cathode	Ni	Zn	$Ni_{0.9}Cr_{0.1}$	Pt	Stainless Steel	Cu
5.0 mA	58	25	40	0	10	0
4.0 mA	60	33	47	0	15	0
3.0 mA	50	22	50	0	17	0
2.0 mA	30	18	44	0	8	0

Solvent \ Catalyst	CuCl	CuBr	CuI	CuCN	$Cu(MeCN)_4BF_4$	$Cu(OTf)_2$
MeCN	60	34	8	0	64	25
DMF	21	15	10	0	18	6
DMAc	33	18	6	0	35	10
DMSO	30	22	4	0	24	8

Catalyst \ Ligand	L1 L7	L2 L8	L3 L9	L4 L10	L5 L11	L6 L12
CuCl	10	0	0	60	0	33
$Cu(MeCN)_4BF_4$	8	0	0	64	0	30
CuCl	42	58	36	44	8	0
$Cu(MeCN)_4BF_4$	45	57	27	42	9	0

Catalyst \ Electrolyte	KBr	$TBABF_4$	$TBAPF_6$	TBAB	$TBAClO_4$	LiBr	
CuCl	60	92	87	72	0	32	L4
$Cu(MeCN)_4BF_4$	58	88	82	75	5	44	
CuCl	64	90	85	77	0	35	L8
$Cu(MeCN)_4BF_4$	57	90	82	61	3	41	

[a]Reaction conditions: **1** (0.05 mmol, 1.0 equiv), Cu(I) (10 mol %), **L** (12 mol %), electrolyte (0.1 mmol, 0.2 M), and solvent (0.5 mL) at 25 °C with 4 mA at 12 h. [b]The yield of **4** was determined by HPLC.

Scheme 3. Scope of Aryl Halide Self-Coupling[a,b]

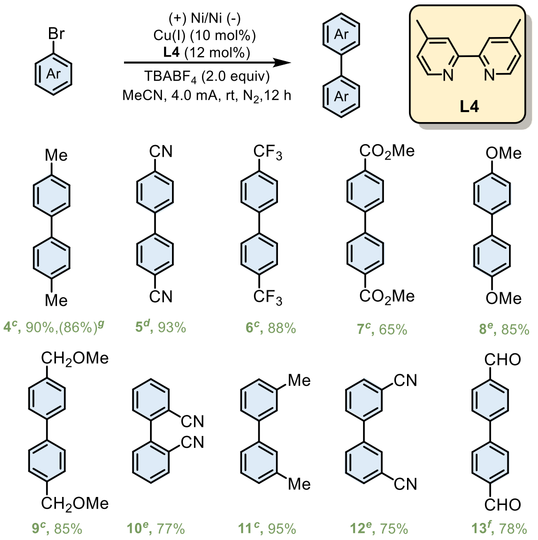

[a]Reaction conditions: **a** (0.5 mmol, 1.0 equiv), Cu(I) (10 mol %), **L4** (12 mol %), $TBABF_4$ (1 mmol, 0.2 M), and MeCN (5 mL) at 25 °C with 4 mA at 12 h. [b]Isolated yields. [c]CuCl (10 mol %) as the catalyst. [d]CuI (10 mol %) as the catalyst. [e]$Cu(MeCN)_4BF_4$ (10 mol %) as the catalyst. [f]CuBr (10 mol %) as the catalyst. [g]**a** (1 mmol).

Scheme 4. Optimization of Ullmann-Type Cross-Coupling[a,b,c]

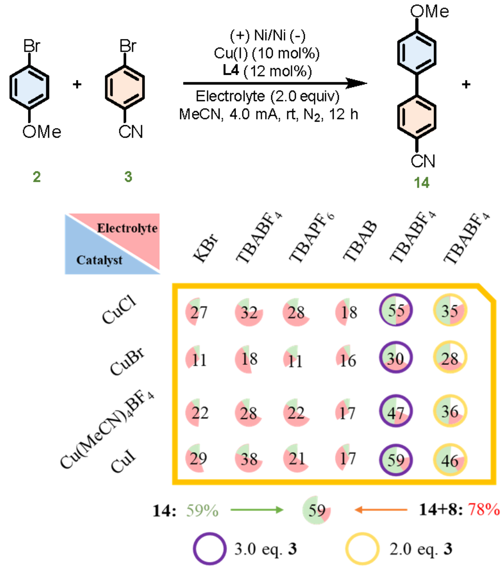

Catalyst \ Electrolyte	KBr	$TBABF_4$	$TBAPF_6$	TBAB	$TBABF_4$	$TBABF_4$
CuCl	27	32	28	18	55	35
CuBr	11	18	11	16	30	28
$Cu(MeCN)_4BF_4$	22	28	22	17	47	36
CuI	29	38	21	17	59	46

[a]Reaction conditions: **2** (0.05 mmol, 1.0 equiv), **3** (0.05 mmol, 1.0 equiv), Cat. (10 mol %), **L4** (12 mol %), electrolyte (0.1 mmol, 0.2 M), and MeCN (0.5 mL) at 25 °C at 12 h. [b]The yields of **8** and **14** were determined by HPLC. [c]The yields of products **8** and **14** were calculated based on substrate **2**.

Scheme 5. Scope of Aryl Halide Cross-Coupling[a,b]

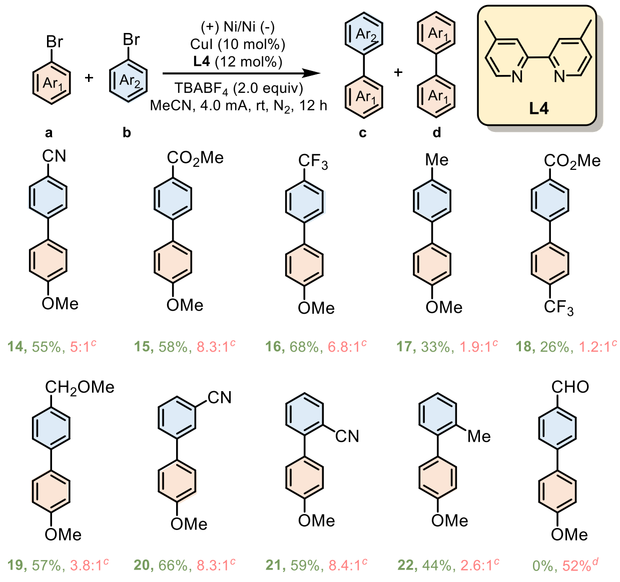

[a]Reaction conditions: **a** (0.5 mmol, 1.0 equiv), **b** (1.5 mmol, 3.0 equiv), CuI (10 mol %), **L4** (12 mol %), $TBABF_4$ (1 mmol, 0.2 M), and MeCN (5 mL) at 25 °C with 4 mA at 12 h. [b]Isolated yields. [c]Ratios between **c** and **d**. [d]Yield of **d**.

the reaction failed to proceed with the substrate containing an active aldehyde group. In summary, this reaction demonstrates a certain level of generality across substrates containing different types and positions of functional groups with a satisfactory chemoselectivity of up to 8.4:1.

Following the chemoselective cross-coupling, the possibility of an enantioselectivity-controlling synthesis was explored. With 2-bromo-3,4,5-trimethoxybenzaldehyde as a model substrate and a series of chiral bidentate nitrogen ligands, an enantioselective product was successfully achieved. The reaction conditions were subsequently optimized to improve the reaction efficiency and enantioselectivity (some representative examples presented in Scheme 6), resulting in an enantiomeric ratio (*e.r.*) of 92.5:7.5 and a 72% isolated yield. The absolute configuration of **24** was confirmed as *S*-type by the literature.[10] Further efforts on substrate scope expansion were devoted, exhibiting some improvement in enantioselectivity control compared with existing reports (Scheme 7). However, naphthaldehyde (**31**) was found to not be a suitable substrate for enantioselective self-coupling in this system. Replacing the aldehyde groups with benzyloxy substituents was an effective approach to get over this hurdle, achieving an *e.r.* value of 88.5:11.5 and a yield of 65% (**32**).

Scheme 6. Optimization of Enantioselective Coupling[a,b,c]

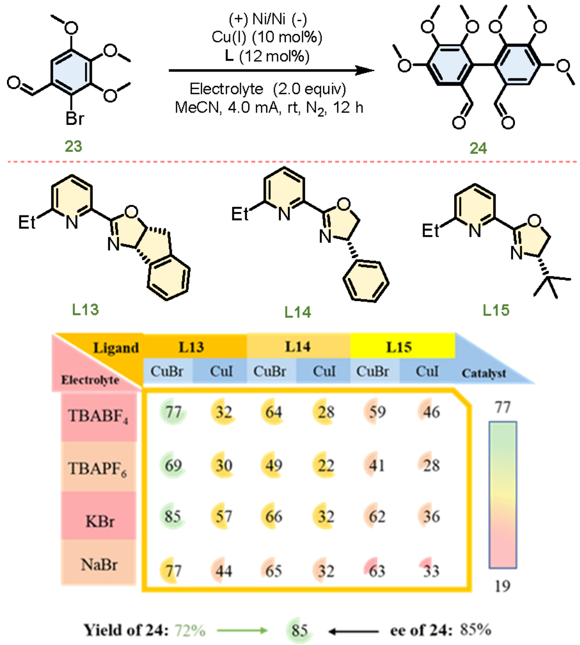

Electrolyte \ Ligand	L13		L14		L15	
	CuBr	CuI	CuBr	CuI	CuBr	CuI
$TBABF_4$	77	32	64	28	59	46
$TBAPF_6$	69	30	49	22	41	28
KBr	85	57	66	32	62	36
NaBr	77	44	65	32	63	33

[a]Reaction conditions: **23** (0.05 mmol, 1.0 equiv), CuBr (10 mol %), **L13** (12 mol %), KBr (0.1 mmol, 0.2 M), and MeCN (0.5 mL) at 25 °C with 4 mA at 12 h. [b]Enantioselectivities were determined by chiral HPLC analysis. [c]Yields were determined by HPLC.

Some mechanistic insights were first sought through cyclic voltammetry analysis of the reaction system (Figure 1).[14] No obvious peak was observed with a solution of CuBr (curve b). The reduction potential of the ligand was measured as −2.66 V (relative to Ag/$AgNO_3$) with only the ligand added to the system (curve c). A mixture of the catalyst and ligand exhibited a notable reduction peak at −1.97 V, indicating that the reduction potential of the ligand increased after coordinating with copper (curve d). Subsequently, introducing the full set of reactants (curve f) preserved this reduction peak at −1.97 V and unveiled additional reduction peaks at −2.08, −2.53, and −2.72 V. These observations led us to speculate that the origin of these new peaks was attributed to the spontaneous oxidative addition reduction between Cu(I) complex and aryl halides, and the resulting Cu(III) complex could be easily reduced with multistep dynamics by the cathode in this electrocatalytic system. To delve deeper into the mechanistic aspects of the reaction, we then performed radical trapping experiments as

Scheme 7. Aryl Halogenated Aldehydes Enantioselectively Conjugate Substrates[a,b,c]

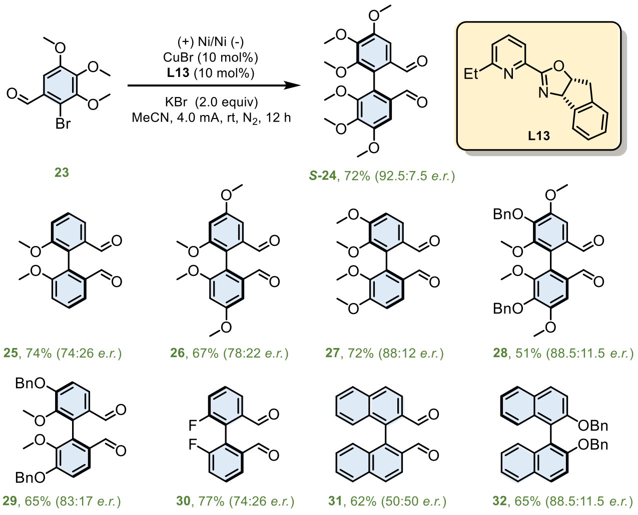

23

S-24, 72% (92.5:7.5 e.r.)

25, 74% (74:26 e.r.)

26, 67% (78:22 e.r.)

27, 72% (88:12 e.r.)

28, 51% (88.5:11.5 e.r.)

29, 65% (83:17 e.r.)

30, 77% (74:26 e.r.)

31, 62% (50:50 e.r.)

32, 65% (88.5:11.5 e.r.)

[a]Reaction conditions: **23** (0.05 mmol, 1.0 equiv), CuBr (10 mol %), **L13** (12 mol %), KBr (0.1 mmol, 0.2 M), and MeCN (0.5 mL) at 25 °C with 4 mA at 12 h. [b]Enantioselectivities were determined by chiral HPLC analysis. [c]Isolated yield.

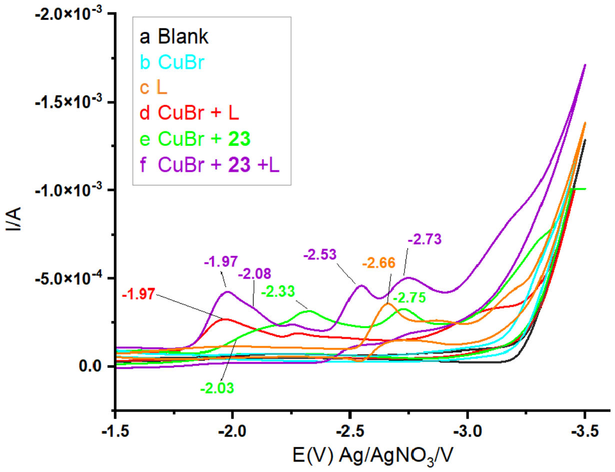

Figure 1. Cyclic voltammograms recorded on a glassy carbon electrode (area = 0.03 cm^2) with a scan rate of 100 mV s^{-1} and a MeCN solution containing 0.1 M n-Bu$_4$NPF$_6$ and (a) none; (b) 2.5 mM CuBr; (c) 2.5 mM **L4**; (d) 2.5 mM CuBr and 2.5 mM **L4**; (e) 2.5 mM CuBr and 2.5 mM **23**; (f) 2.5 mM CuBr, 2.5 mM **L4**, and 2.5 mM **23**.

Scheme 8. Radical Trapping Experiment

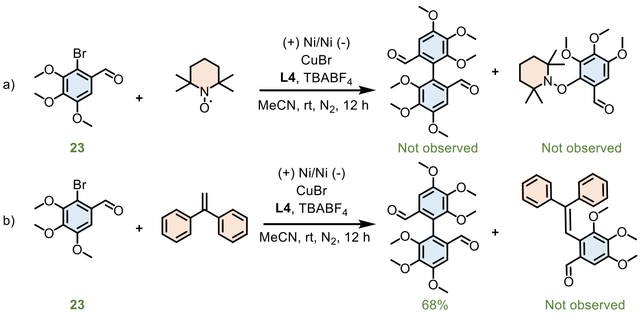

illustrated in Scheme 8. Our initial approach involved incorporating the radical scavenger 2,2,6,6-tetramethyl-1-piperidinyloxy (TEMPO) into the reaction milieu (Scheme 8a). The presence of TEMPO resulted in a marked inhibition of the reaction yet no radical-adduct product was identified, suggesting that the oxidative structure of TEMPO may impede the reaction's progress. To circumvent potential oxidative interference, we subsequently employed 1,1-diphenylethylene, a scavenger of neutral redox character, in our experimental setup (Scheme 8b). This modification allowed the reaction to proceed unimpeded (isolated yield of 68%) and did not yield any evidence of radical capture. Based on these outcomes, we propose that the reaction pathway likely does not involve the participation of free radical intermediates. Further investigations on the influence of the Ni electrodes were conducted with several control experiments, demonstrating the reaction is reliably catalyzed by the copper catalyst instead of the dissociative nickel from the electrodes (for details, see Tables S12 and S13).

Drawing from the corpus of existing literature[12,15] and our experimental data, a proposed catalytic mechanism for this reaction is depicted in Scheme 9. The process begins with the formation of metal complex **A** from the catalyst and ligand initially introduced. An oxidative addition between **A** and halogenated aromatics forms Cu(III) species **B**, and a following two-electron reduction at the cathode transfers **B** to Cu(I) species **C**. Then species **C** undergoes a second oxidative addition with another molecule of aryl halides to form Cu(III) species **D**. Finally, the biaryl product is afforded through reduction elimination of complex **D** and regenerated Cu(I) complex **A** will enter the next cycle.

Scheme 9. Proposed Mechanism

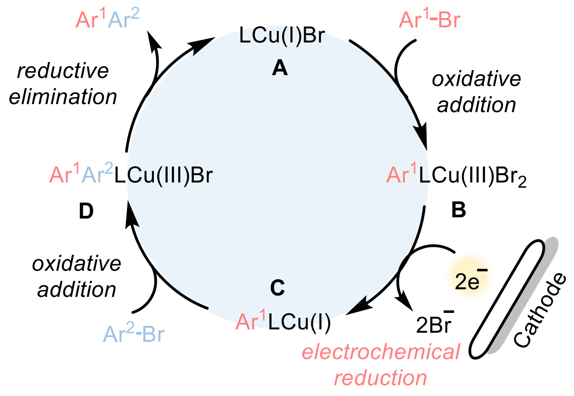

In summary, we have developed a copper-electrocatalyzed method to selectively synthesize biaryl aromatic scaffolds. This approach encompasses halogenated aromatic self-coupling, chemoselective coupling of halogenated aromatics, and enantioselective homocoupling of halogenated aryl aldehydes. Notably, the method eliminates the need for organometallic reagents and circumvents the use of stoichiometric reducing agents. The reaction conditions are mild, and through high-throughput screening techniques, optimal conditions are rapidly identified, offering a viable route to expedite the experimental cycle in electrochemical synthesis. Research on the electrocatalytic synthesis of biaryl aromatic frameworks and related experimental studies is ongoing, further expanding the application of this innovative approach.

■ ASSOCIATED CONTENT

Data Availability Statement

The data underlying this study are available in the published article and its Supporting Information.

Supporting Information

The Supporting Information is available free of charge at https://pubs.acs.org/doi/10.1021/acs.orglett.4c03196.

Experimental details and characterization data (PDF)

■ AUTHOR INFORMATION

Corresponding Authors

Yunhe Jin − *School of Chemistry, Dalian University of Technology (DUT), Dalian 116081, China;* orcid.org/0000-0003-0626-4587; Email: jinyh18@dlut.edu.cn

Shengyang Tao − *School of Chemistry, Dalian University of Technology (DUT), Dalian 116081, China;* orcid.org/0000-0002-0567-8860; Email: taosy@dlut.edu.cn

Authors

Yun Zou − *School of Chemistry, Dalian University of Technology (DUT), Dalian 116081, China*

Jia Xin − *School of Chemistry, Dalian University of Technology (DUT), Dalian 116081, China*

Complete contact information is available at: https://pubs.acs.org/10.1021/acs.orglett.4c03196

Notes

The authors declare no competing financial interest.

■ ACKNOWLEDGMENTS

This work was supported by the National Natural Science Foundation of China (No. 22372025), the Fundamental Research Funds for the Central Universities (No. DUT22-LAB607, DUT22QN226), the Projects of International Cooperation and Exchanges NSFC-BRFFR (No. 22211530456), and Project 1912 Funds.

■ REFERENCES

(1) Bringmann, G.; Gulder, T.; Tobias, A. M.; Gulder, T. A. M.; Breuning, M. Atroposelective total synthesis of axially chiral biaryl natural products. *Chem. Rev.* **2011**, *111*, 563−639.

(2) (a) Yoon, T. P.; Jacobsen, E. N. Privileged Chiral Catalysts. *Science* **2003**, *299*, 1691−1693. (b) Terada, M. Chiral Phosphoric Acids as Versatile Catalysts for Enantioselective Transformations. *Synthesis* **2010**, *2010*, 1929−1982.

(3) Zhang, X.; Yang, X.; Rong, Q.; Liu, X.; Zhou, Y.; Yang, H.; Wang, G.; Chen, Z.; Wang, X. *ACS ES&T Engineering* **2024**, *4*, 250−268.

(4) For selected recent examples, see: (a) Shen, D.; Xu, Y.; Shi, S.-L. A Bulky Chiral N-Heterocyclic Carbene Palladium Catalyst Enables Highly Enantioselective Suzuki−Miyaura Cross-Coupling Reactions for the Synthesis of Biaryl Atropisomers. *J. Am. Chem. Soc.* **2019**, *141*, 14938−14945. (b) Xu, G.; Fu, W.; Liu, G. D.; Senanayake, C. H.; Tang, W. Efficient syntheses of korupensamines A, B and michellamine B by asymmetric Suzuki-Miyaura coupling reactions. *J. Am. Chem. Soc.* **2014**, *136*, 570−573. (c) Shen, X.; Jones, G. O.; Watson, D. A.; Bhayana, B.; Buchwald, S. L. Enantioselective synthesis ofaxially chiral biaryls by the Pd-catalyzed Suzuki-Miyaura reaction:Substrate scope and quantum mechanical investigations. *J. Am. Chem. Soc.* **2010**, *132*, 11278−11287. (d) Zhang, S.-S.; Wang, Z.-Q.; Xu, M.-H.; Lin, G.-Q. Chiral diene as the ligand for the synthesis of axiallychiral compounds via palladium-catalyzed Suzuki-Miyaura couplingreaction. *Org. Lett.* **2010**, *12*, 5546−5549.

(5) (a) Tian, J.-M.; Wang, A.-F.; Yang, J.-S.; Zhao, X.-J.; Tu, Y.-Q.; Zhang, S.-Y.; Chen, Z.-M. Copper-Complex-Catalyzed Asymmetric Aerobic Oxidative Cross-Coupling of 2-Naphthols: Enantioselective Synthesis of 3,3′-Substituted C1-Symmetric BINOLs. *Angew. Chem., Int. Ed.* **2019**, *58*, 11023−11027. (b) Kang, H.; Herling, M. R.; Niederer, K. A.; Lee, Y. E.; Reddy, P. V. G.; Dey, S.; Allen, S. E.; Sung, P.; Hewitt, K.; Torruellas, C.; Kim, G. J.; Kozlowski, M. C. Enantioselective Vanadium-Catalyzed Oxidative Coupling: Development and MechanisticInsights. *J. Org. Chem.* **2018**, *83*, 14362−14384. (c) Narute, S.; Parnes, R.; Toste, F. D.; Pappo, D. Enantioselective Oxidative Homocoupling and Cross-Coupling of 2-Naphthols Catalyzed by Chiral Iron Phosphate Complexes. *J. Am. Chem. Soc.* **2016**, *138*, 16553−16560.

(6) For selected recent examples, see: (a) Kang, K.; Loud, N. L.; DiBenedetto, T. A.; Weix, D. J. A General, Multimetallic Cross-Ullmann Biheteroaryl Synthesis from Heteroaryl Halides and Heteroaryl Triflates. *J. Am. Chem. Soc.* **2021**, *143*, 21484−21491. (b) Kang, K.; Huang, L.; Daniel, J. W. Sulfonate Versus Sulfonate: Nickel and Palladium Multimetallic Cross-Electrophile Coupling of Aryl Triflates with Aryl Tosylates. *J. Am. Chem. Soc.* **2020**, *142*, 10634−10640.

(7) Ullmann, F.; Bielecki, J. Ueber Synthesen in der Biphenylreihe. *Ber. Dtsch. Chem. Ges.* **1901**, *34*, 2174.

(8) (a) Sainsbury, M. Modern methods of aryl-aryl bond formation. *Tetrahedron* **1980**, *36*, 3327. (b) Jukes, A. E. The Organic Chemistry of Copper. *Adv. Organoment. Chem.* **1974**, *12*, 215. (c) Wu, T.-F.; Zhang, Y.-J.; Fu, Y.; Liu, F.-J.; Tang, J.-T.; Liu, P.; Toste, F. D.; Ye, B. Zirconium-redox-shuttled cross-electrophile coupling of aromatic and heteroaromatic halides. *Chem.* **2021**, *7*, 1963−1974.

(9) Li, Y.; Yin, G. Bathocuproine-Enabled Nickel-Catalyzed Selective Ullmann Cross-Coupling of Two sp^2-Hybridized Organohalides. *Synlett* **2021**, *32*, 1657−1661.

(10) Chen, W.-W.; Zhao, Q.; Xu, M.-H.; Lin, G.-Q. Nickel-catalyzed Asymmetric Ullmann Coupling for the Synthesis of Axially Chiral Tetra-ortho-substituted Biaryl Dials. *Org. Lett.* **2010**, *12*, 1072−1075.

(11) (a) Horn, E. J.; Rosen, B. R.; Baran, P. S. Synthetic organic electrochemistry: an enabling and innately sustainable method. *ACS Cent Sci.* **2016**, *2*, 302−308. (b) Yan, M.; Kawamata, Y.; Baran, P. S. Synthetic organic electrochemical methods since 2000: on the verge of a renaissance. *Chem. Rev.* **2017**, *117*, 13230−319. (c) Ma, C.; Fang, P.; Liu, Z.-R.; Xu, S.-S.; Xu, K.; Cheng, X.; Lei, A.; Xu, H.-C.; Zeng, C.; Mei, T.-S. Recent advances in organic electrosynthesis employing transition metal complexes as electrocatalysts. *Sci. Bull.* **2021**, *66*, 2412−2429. (d) Zhang, B.; Gao, Y.; Hioki, Y.; Oderinde, M. S.; Qiao, J. X.; Rodriguez, K. X.; Zhang, H.-J.; Kawamata, Y.; Baran, P. S. Ni-Electrocatalytic C(sp3)−C(sp3) Doubly Decarboxylative Coupling. *Nature* **2022**, *606*, 313−318. (e) Li, P.; Zhu, Z.; Guo, C.; et al. Nickel-electrocatalysed C(sp^3)−C(sp^3) cross-coupling of unactivated alkyl halides. *Nat. Catal.* **2024**, *7*, 412−421.

(12) For selected recent examples, see: (a) Qiu, H.; Shuai, B.; Wang, Y.-Z.; Liu, D.; Chen, Y.-G.; Gao, P.-S.; Ma, H.-X.; Chen, S.; Mei, T.-S. Enantioselective Ni-Catalyzed Electrochemical Synthesis of Biaryl Atropisomers. *J. Am. Chem. Soc.* **2020**, *142*, 9872−9878. (b) Wang, Y.-Z.; Sun, B.; Zhu, X.-Y.; Gu, Y.-C.; Ma, C.; Mei, T.-S. Enantioselective Reductive Cross-Couplings of Olefins by Merging Electrochemistry with Nickel Catalysis. *J. Am. Chem. Soc.* **2023**, *145*, 23910−23917.

(13) Rein, J.; Annand, J. R.; Wismer, M. K.; Fu, J.; Siu, J. C.; Klapars, A.; Strotman, N. A.; Kalyani, D.; Lehnherr, D.; Lin, S. Unlocking the Potential of High-Throughput Experimentation for Electrochemistry with a Standardized Microscale Reactor. *ACS Cent. Sci.* **2021**, *7*, 1347−1355.

(14) Song, L.; Fu, N.; Ernst, B. G.; et al. Dual electrocatalysis enables enantioselective hydrocyanation of conjugated alkenes. *Nat. Chem.* **2020**, *12*, 747−754.

(15) (a) Yu, H.; Jiang, Y.; Fu, Y.; Liu, L. Alternative Mechanistic Explanation for Ligand-Dependent Selectivities in Copper-Catalyzed

N- and *O*-Arylation Reactions. *J. Am. Chem. Soc.* **2010**, *132*, 18078−18091. (b) Lefevre, G.; Franc, G.; Adamo, C.; Jutand, A.; Ciofini, I. Influence of the Formation of the Halogen Bond ArX- - -N on the Mechanism of Diketonate Ligated Copper-Catalyzed Amination of Aromatic Halides. *Organometallics* **2012**, *31*, 914−920.

https://doi.org/10.1021/acs.orglett.4c03196